Published in Journal of Molecular Biology 356, issue 3, 738-745, 2006
which should be used for any reference to this work

Crystallographic Analysis of a Full-length Streptavidin with Its C-terminal Polypeptide Bound in the Biotin Binding Site

Isolde Le Trong[1], Nicolas Humbert[2], Thomas R. Ward[2] and Ronald E. Stenkamp[1]*

[1]*Departments of Biological Structure and Biochemistry and the Biomolecular Structure Center, University of Washington, Box 357420 Seattle, WA 98195-7420, USA*

[2]*Institute of Chemistry University of Neuchâtel Neuchâtel CH-2000 Switzerland*

**Corresponding author*

The structure of a full-length streptavidin has been determined at 1.7 Å resolution and shows that the 20 residue extension at the C terminus forms a well-ordered polypeptide loop on the surface of the tetramer. Residues 150–153 of the extension are bound to the ligand-binding site, possibly competing with exogenous ligands. The binding mode of these residues is compared with that of biotin and peptidic ligands. The observed structure helps to rationalize the observations that full-length mature streptavidin binds biotinylated macromolecules with reduced affinity.

Keywords: full-length streptavidin; crystallography; self-binding; protein/ligand interactions

Introduction

Streptavidin binds biotin with high affinity ($K_d \sim 10^{-13}$ M).[1] This makes it of considerable use in biotechnical applications involving labeling and transport of biochemical reagents. The tight binding between streptavidin and biotin is also the subject of biophysical, structural and computational investigations probing the nature of the protein–ligand interactions.[2–5]

Streptavidin, after expression in *Streptomyces avidinii* as a polypeptide of 159 residues, is rapidly cleaved by proteases to yield several truncated versions of the protein.[6] The most stable and well-studied form of the protein contains residues 13–139 and is called core-streptavidin. The crystal structure of core streptavidin,[7,8] showed that the protein is a tetramer with D_2 symmetry. Each subunit contains a β-barrel structure with a biotin-binding site located at one end of the barrel.

The biotin-binding site is made up of several hydrogen bonding amino acid side-chains (N23, S27, Y43, S45, and D128) as well as several tryptophan residues (W79, W92, W108, and W120 (from a neighboring subunit)). There are extensive subunit–subunit interactions in the tetramer, and each biotin site contains residues from two subunits. In addition, a flexible binding loop (residues 45–52) undergoes a conformational change upon ligand binding and closes over the binding site, nearly burying it from the aqueous environment.

Streptavidin/ligand interactions have been probed both by mutating the protein[5,9,10] and by varying the structure of the ligand.[11–14] These studies have been driven by theoretical as well as biotechnical considerations, and a number of crystal structures of streptavidin and its ligands are available in the Protein Data Bank.

Streptavidin exists in a number of forms in *S. avidinii*.[6] These appear to be cleavage products of the 159 residue form termed mature, full-length streptavidin. Several reports suggest that streptavidins truncated at the C terminus display enhanced binding affinity for large biotinylated macromolecules.[6,15] To date, no crystallographic structural information for the full-length streptavidin has been available to explain this reduced affinity.

In recent years, one of us has reported on the use of mature streptavidin as a host protein for biotinylated organometallic catalyst precursors. Such artificial metalloenzymes show promising properties as hybrid catalysts for enantioselective hydrogenation and transfer hydrogenation reactions.[16–18] With the aim of solving the X-ray structure of such artificial metalloenzymes, we have solved the structure of unliganded, full-length

Abbreviations used: T7-SA, T7 tagged streptavidin; PDB, Protein Data Bank.

E-mail address of the corresponding author: stenkamp@u.washington.edu

Table 1. Diffraction data statistics

Resolution shells (Å)	Number reflections	⟨*I*⟩	Error	Redundancy	% Complete	Norm. χ^2	R_{merge}
50.0–3.30	4556	285,687.5	13,809.4	4.2	98.6	0.947	0.054
3.30–2.62	4552	110,429.5	5318.9	4.2	99.7	1.086	0.060
2.62–2.29	4544	44,891.6	2462.8	4.1	99.8	0.987	0.062
2.29–2.08	4532	31,710.9	1845.6	4.0	99.7	1.169	0.068
2.08–1.93	4515	19,061.8	1376.5	4.0	99.7	1.155	0.085
1.93–1.81	4504	9384.7	873.5	4.0	100.0	1.156	0.119
1.81–1.72	3938	4754.1	579.7	3.5	86.5	1.321	0.160
1.72–1.65	2528	2568.2	452.1	2.9	55.9	1.430	0.216
1.65–1.68	1394	1461.1	363.0	2.4	30.7	1.514	0.259
1.58–1.53	318	1039.5	355.2	1.7	7.1	1.483	0.270
Overall	35,381	65,229.5	3416.4	3.8	77.9	1.131	0.061

streptavidin at 1.7 Å resolution. The protein construct, designated T7-SA, is 159 residues long with the first 13 residues of streptavidin being replaced by a T7 epitope tag†. The C-terminal extension beyond residue 139, the normal core-streptavidin terminus, folds back on the protein and occupies the biotin-binding site. Here we describe the structure of this self-binding streptavidin.

Results and Discussion

Data set and refinement statistics for the T7-SA crystal structure are presented in Tables 1 and 2. The data set used in refinement has an effective resolution of about 1.7 Å. While reflections to 1.53 Å resolution were used in the refinement, the outer shells of data are not complete, presumably due to the shape of the detector. The effect of this on the refinement and the resulting electron density maps is not known, but it seems unlikely to affect the overall structure in significant ways.

Two T7-SA subunits are found in the asymmetric unit of the unit cell reported here, but the crystal actually contains streptavidin tetramers possessing 222 (D_2) symmetry. They have arranged themselves in the crystal with one of the tetrameric 2-fold rotation axes coinciding with a crystallographic 2-fold axis in the *C*2 space group. One of the non-crystallographic 2-fold axes in the tetramer is parallel to the *a* axis of the unit cell. This, coupled with the C-centering operation of the space group, results in layers of tetramers in the *a*–*b* plane of the unit cell, with their third 2-fold rotation axis (again non-crystallographic) perpendicular to the layers. Adjacent layers are packed such that the 2-fold rotation axes for one layer do not align with those of the neighboring layer. Thus, these 2-folds must be non-crystallographic, and the space group must be the monoclinic *C*2.

In T7-SA, the 13 N-terminal residues of full-length streptavidin have been replaced by the T7-tag known to solubilize recombinant proteins (see Figure 1). In this crystal form, no electron density is observed for the T7-tag. Core-streptavidin, the most common form of the protein used in research and technical applications, is comprised of residues 13–139, and is 20 amino acid residues shorter than the full-length molecule at the C terminus.[6] Electron density is seen in the T7-SA crystal for residues 12 and 13 in one subunit, but not in the second. The density for the N-terminal residues is not strong, indicating the presence of static or dynamic disorder in this part of the structure. T7-SA contains the C-terminal extension and much of it is observed in each of the two subunits in the asymmetric unit.

The structure of the streptavidin tetramer is shown in Figure 2. The overall folding topology of one of the unique T7-SA protomers in this crystal structure is shown in blue in Figure 2. The fundamental β-barrel fold found in other streptavidin monomers in other crystal structures is found in T7-SA as well. When compared to core-streptavidin, one additional residue is seen at the N terminus while 20 additional residues are seen at the C terminus (17 in the second molecule in the asymmetric unit). The C-terminal extension stretches away from the β-barrel, forms a section

Table 2. Refinement statistics

Resolution range (Å) (but reflections to 1.53 Å included in the refinement)	10.0–1.7
Number of unique reflections	35,214
Number of reflections in working set	31,693
Number of reflections in working set with $\|F_o\| > 4\sigma(\|F_o\|)$	29,622
Number of reflections in test set	3521
Number of reflections in test set with $\|F_o\| > 4\sigma(\|F_o\|)$	3296
Number of parameters	9763
Number of restraints	6886
R_{work} (all reflections)	0.175
R_{work} ($\|F_o\| > 4\sigma(\|F_o\|)$)	0.171
R_{free} (all reflections)	0.244
R_{free} ($\|F_o\| > 4\sigma(\|F_o\|)$)	0.236
R_{final} (all reflections)	0.179
R_{final} ($\|F_o\| > 4\sigma(\|F_o\|)$)	0.176
Goodness of fit	4.157
Number of protein atoms	2151
Number of solvent atoms	279
Number of heteroatoms	15
Mean *B* value (isotropic) (Å^2)	44.2
Main-chain atoms	42.7
Side-chain atoms	44.2
Solvent and heteroatoms	52.7
r.m.s. deviations from ideal bond lengths (Å)	0.010
r.m.s. deviations from ideal bond angles (Å)	0.028

† http://www.merckbiosciences.co.uk/docs/docs/PROT/TB055.pdf

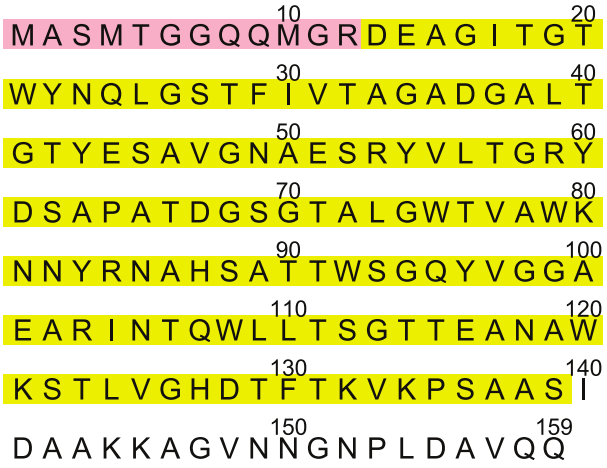

Figure 1. The amino acid sequence of T7 tagged mature streptavidin. The T7 tag is used to increase the solubility of recombinant proteins and replaces the 13 N-terminal residues of full-length streptavidin in this construct. The T7 tag is highlighted in magenta. The sequence of core-streptavin (residues 13–139) is highlighted in yellow.

of α-helix, and then folds against the β-barrel with several residues located within the biotin-binding site.

The C-terminal extension does not alter the fundamental subunit interactions leading to the streptavidin tetramer (see Figure 2). The additional residues are located away from neighboring subunits and do not interact with any of them, including subunits within the tetramer and subunits in adjacent tetramers in the crystal.

The major structural element of the C-terminal extension is a 12 residue long α-helix. The tracing of the polypeptide as shown in Figure 2 suggests that the helix is loosely connected with the rest of the protein structure. Figure 3 shows that the region between the helix and the β-barrel is filled with side-chains from several residues. These are largely hydrophobic residues, consistent with this region being part of a typical globular protein.

In fact, the additional residues for full-length streptavidin are simply appended to the fundamental protein fold of core-streptavidin. Figure 4 shows the superposition of a subunit of wild-type core-streptavidin (in complex with biotin) (PDB ident 1MK5) on a T7-SA subunit. The major difference in the polypeptide folds for the two molecules is in the flexible binding loop near residues 45–52. In the wild-type biotin complex, this loop folds over the bound ligand. In the T7-SA structure, the loop remains flexible in the open position (as found in wild-type core-streptavidin), flexible enough that electron density is not seen for several of the residues in the loop.

A smaller conformational difference between T7-SA and core-streptavidin is seen near residues 24–26 (see Figure 5). These residues in T7-SA are shifted as much as 2.5 Å from their positions in core-streptavidin, possibly to maximize hydrophobic contacts with the C-terminal helix and neighboring residues. The movement appears to be a semi-rigid rotation of that loop away from the ligand-binding site.

The novel characteristic of this crystal structure is the presence of residues 150–153 at the C-terminal end of the polypeptide in the biotin-binding site. These residues occupy a larger volume than does biotin, so the flexible loop (residues 45–52) is not able to fold over the binding site as it does in the biotin complex with wild-type core-streptavidin.

Among the many streptavidin-ligand complexes in the Protein Data Bank several contain small exogenous peptides in the biotin site. Visual inspection of 30 of these complexes confirms that they bind to the biotin site in streptavidin in similar ways. PDB entry 1VWL[13] is typical of this class of complexes. Figure 6 shows the superposition of T7-SA with the wild-type biotin complex and the 1VWL peptide complex. The polypeptide traces for the C-terminal residues of T7-SA and the HPQ peptide from 1VWL are quite different.

The interactions between the ligands (C-terminal residues, biotin or HPQ peptide) and the binding site vary from ligand to ligand, except for one hydrogen bond. The overlap of the three ligands is shown, as well as two hydrogen bonding interactions of particular interest, in Figure 7. In all three complexes, there is a hydrogen bond between the

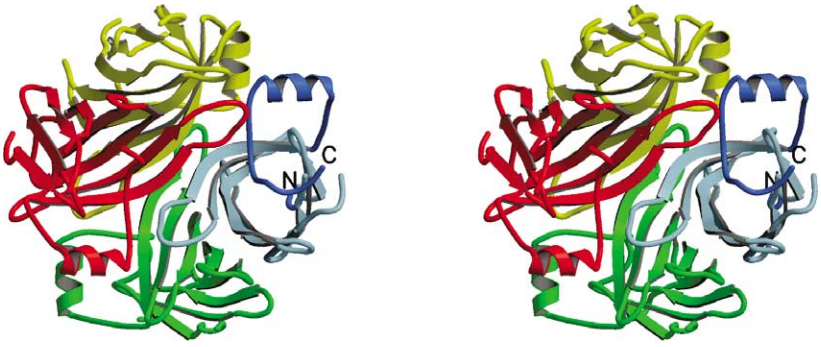

Figure 2. Stereo view of the T7-SA tetramer showing the quaternary structure as well as the overall folding topology and β-barrel fold of the T7-SA subunit. In the blue subunit, the residues corresponding to core-streptavidin are shown in light blue while the additional residues at the N and C terminus are in dark blue. At the C terminus, the polypeptide forms an α-helical segment before folding to place several residues in the biotin-binding pocket. The additional residues at the C terminus do not alter the subunit interactions involved in formation of the streptavidin tetramer.

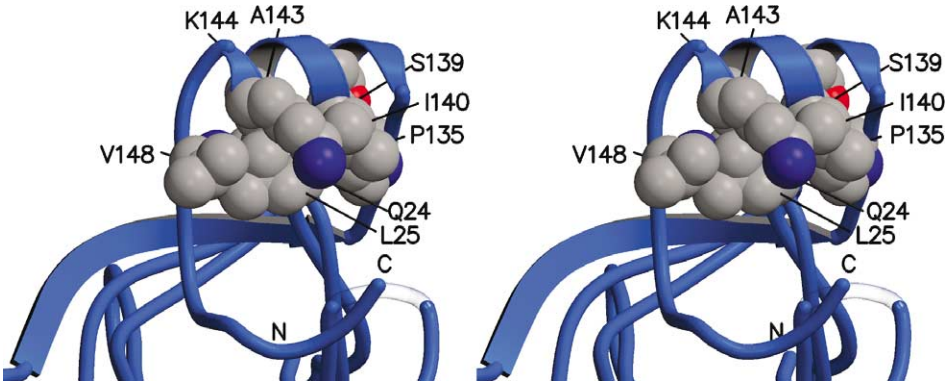

Figure 3. Stereo view of the C-terminal extension in the T7-SA protomer (blue backbone tracing). The space between the helix and the β-barrel is filled with amino acid side-chains with non-hydrogen atoms shown as van der Waals spheres.

ligand and OG1 of Thr90. In the case of T7-SA, the hydrogen bond acceptor is the carbonyl oxygen of Gly151. For the biotin complex, the acceptor is the sulfur atom, and for 1VWL, the acceptor is OE1 of Gln5. The other hydrogen bond shown in Figure 7 involves the OG of Ser88. It interacts with the valeric acid carboxylate in biotin and NE2 of His3 in the peptide complex. In T7-SA, a proline occupies the space occupied by the carboxylate in biotin, and no hydrogen bond is formed with Ser88.

Further analysis of the interactions in T7-SA between the C-terminal residues and the rest of the subunit shows that very few hydrogen bonds are involved. Table 3 lists the possible hydrogen bonds in this part of the subunit structure. The bulk of the hydrogen bond acceptors and donors in the

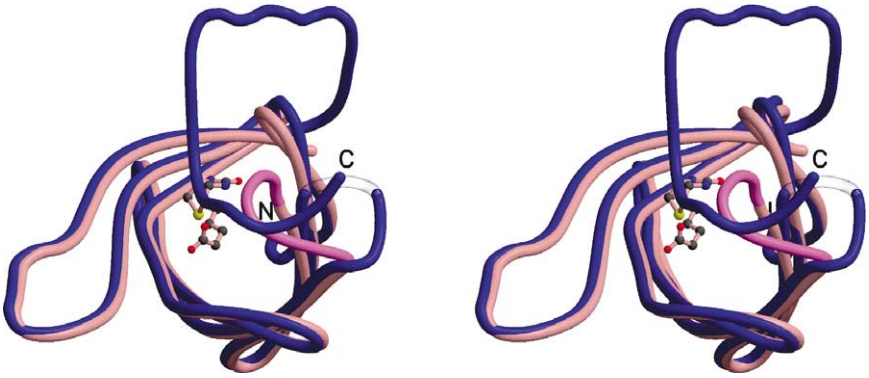

Figure 4. Stereo view of a subunit of wild-type core-streptavidin (PDB ident 1MK5) (pink coil) superposed on T7-SA (blue coil). Biotin (bound in core-streptavidin) is shown in ball-and-stick representation. The flexible binding loop in the biotin complex is shown in violet. The missing residues in this loop in the open conformation in T7-SA are shown as transparent coil. The major differences between the wild-type and T7-SA structures, in addition to the additional residues at the C terminus, involve the conformation of the flexible binding loop (residues 45–52) and the conformation of residues 24–26 near the α helix.

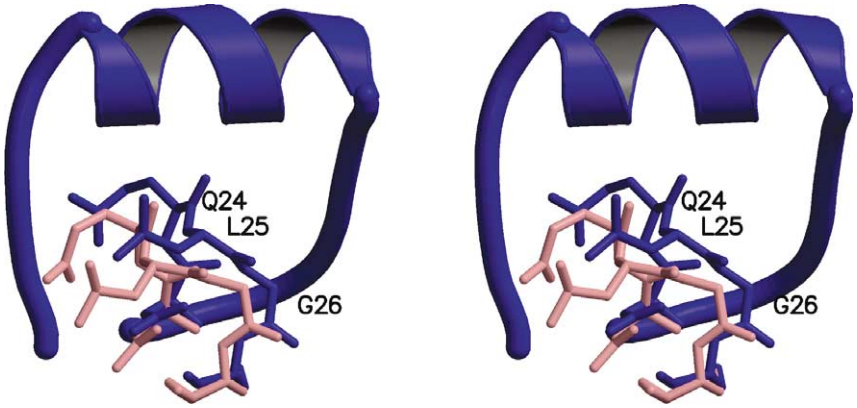

Figure 5. Stereo view showing the differences in the loop containing residues 24–26 in wild-type core-streptavidin (pink) and T7-SA (blue). These residues shift in T7-SA in response to the additional residues at the C-terminal end of the polypeptide. The residues appear to shift as a rigid unit.

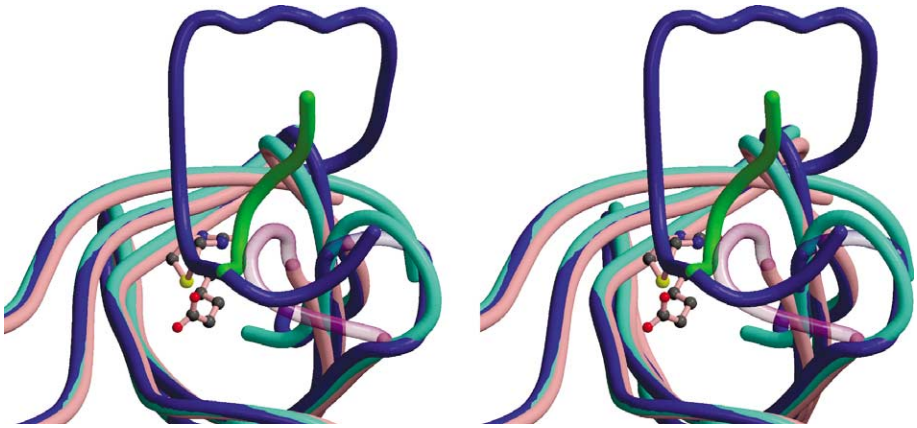

Figure 6. Stereo view of the superposition of the polypeptide tracings of the subunits of T7-SA (blue coil), the biotin complex of wild-type core-streptavidin (pink) and the peptide complex (PDB ident 1VWL[13]) (light green). The peptide from the complex is shown as green coil. The flexible loop in the wild-type core-streptavidin–biotin complex is in transparent violet while the missing residues in T7-SA are in transparent blue. The protein backbone for the C-terminal residues of T7-SA does not align with the peptide ligand from 1VWL.

C-terminal extension (residues 150–159) interact with other atoms within the extension, not with atoms in the core structure. This might allow this part of the structure to be more flexible and might contribute to its susceptibility to protease cleavage.[6]

The flexible binding loop (residues 45–52) is unable to close over the portions of the C-terminal residues that are located in the biotin-binding site in T7-SA. Steric clashes with the residues in the binding site, as well as adjacent residues, keep the binding loop in the open, flexible position. The electron density for several of the residues in this loop in T7-SA was weak or missing, indicating that portions of the loop are flexible in the crystals.

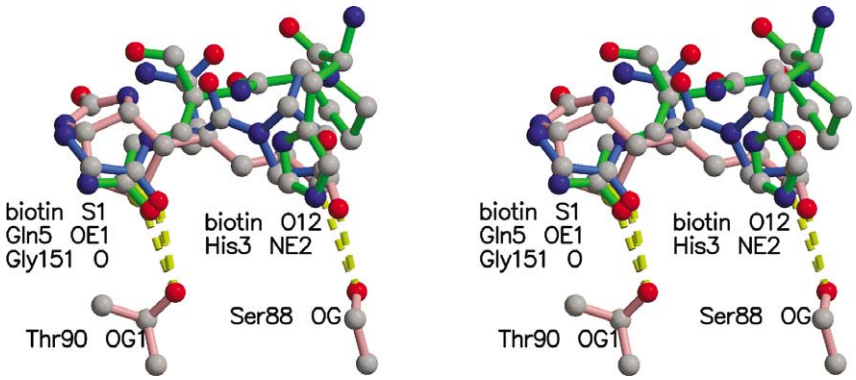

Figure 7. Stereo view of the ligands in the superposed complexes. Residues 151–153 of T7-SA are shown (blue bonds) as are the biotin from the wild-type complex (pink bonds) and the binding residues of the peptide complex (green bonds). All three ligands make a hydrogen bond with OG1 of Thr90.

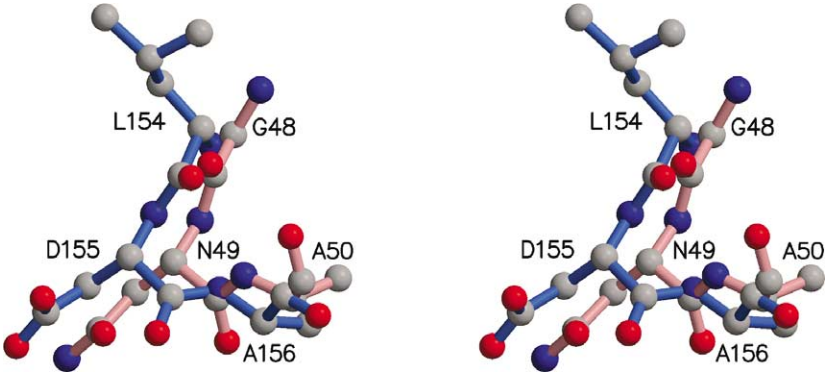

Figure 8. Stereo view showing the overlap of the flexible binding loop in the wild-type core-streptavidin–biotin complex (pink bonds) with residues near the C terminus of T7-SA (blue bonds). Residues 154–156 in T7-SA, while not actually bound in the biotin-binding site, take on the same conformation and nearly the same location as the closed loop in the wild-type–biotin complex.

Table 3. Hydrogen bonds between residues 144–159 of T7-SA and residues 12–143

	Interatomic distance (Å)	
	Chain A	Chain B
Val148 N–Glu117[a] O	3.31	[b]
Asn149 O–Trp108 NE1	2.96	3.17
Gly151 O–Thr90 OG1	2.70	2.75
Asp155 O–Arg84 NH1	2.92	[c]
Asp155 O–Arg84 NE	3.17	[c]
Ala156 O–Tyr54 OH	2.70	[c]
Gln158 N–Ser52 OG	2.78	[d]
Gln158 OE1–Arg84 NH2	3.11	[a]

[a] Residue in the other polypeptide chain in the asymmetric unit.
[b] Residue 117 in chain B modeled as Ala due to lack of electron density.
[c] Side-chain in chain B in a conformation unable to form the hydrogen bond.
[d] Residue 158 not modeled in chain B.

The loop residues that have been located in T7-SA take on the conformation of residues in other streptavidin structures with open loop structures.

While the loop is open in this structure, three residues (Leu154-Asp155-Ala156) just beyond the three residues that mimic the binding of biotin, take on conformations similar to those of the residues in the closed form of the binding loop. Figure 8 shows the overlap of these residues and the closed loop in the biotin complex of wild-type core-streptavidin (PDB ident 1MK5). The three residues (154–156) overlap significantly, both in terms of structure and sequence, with Gly48-Asn49-Ala50 (in the binding loop). Residues 154–156 are translated from the position of the closed loop by 1–2 Å.

No part of the C terminus of T7-SA occupies the pocket where the ureido oxygen of biotin binds in the wild-type core-streptavidin complex. Instead, the pocket is enlarged in T7-SA and is filled by two water molecules (see Figure 9). The water molecules make hydrogen bonds with several of the residues that interact with the ureido oxygen atom and nitrogen atoms of biotin, i.e. Ser27, Tyr43, and Asp128. In addition, the water molecules are hydrogen bonded to Gly151, Asn152, and Trp92. In accommodating the additional volume associated with two water molecules, the binding pocket has expanded. A major component of this expansion is associated with the movement of residues 24–26 as shown in Figure 5.

The structure of T7-SA shows an interesting, unexpected binding interaction between the C-terminal residues of the full-length protein and its biotin-binding site. Whether this binding mode affects the binding of other ligands is not known. Other investigators have shown that full-length streptavidin can bind biotin,[6,19] but quantitative information concerning that interaction is not readily available. The affinity of the C-terminal residues for the biotin site is probably far weaker than that of biotin since biotin makes use of the ureido functional group in its interaction with the protein while the C-terminal residues fail to make use of analogous protein–ligand interactions. It seems unlikely that the C-terminal residues would compete effectively with biotin for the binding site, but it is possible that more weakly bound ligands might display significant binding differences for core and full-length streptavidins.

As stated in the Introduction, full-length streptavidin shows reduced binding of biotinylated macromolecules[6,15] compared with the binding characteristics of core-streptavidin. The structure of T7-SA shows that the additional residues at the C-terminal end of the polypeptide produce an α-helical segment and an extended peptide that binds directly to the ligand-binding site. Since full-length mature streptavidin can bind biotin, residues 150–159 must be flexible enough to allow them to move from the binding site and permit binding. The helical structure does not appear to be blocking access to the binding site for small ligands, but, as pointed out by Bayer *et al.*,[15] it might be sufficient to keep larger molecules from getting close enough to

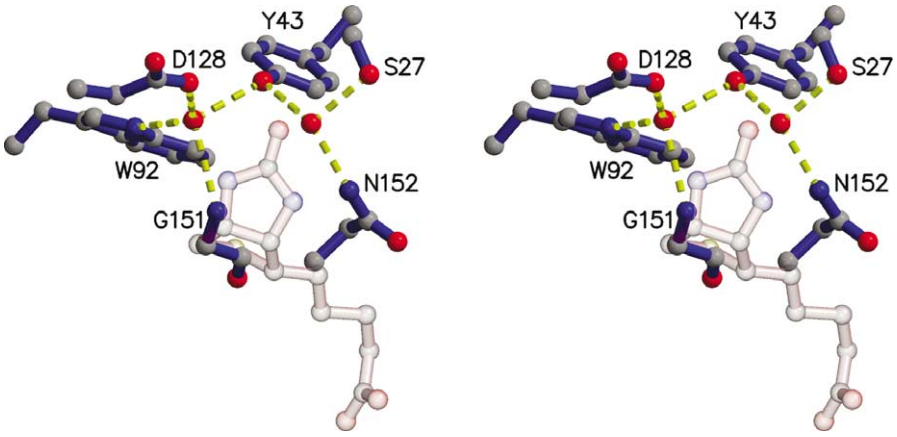

Figure 9. Stereo view of two water molecules in T7-SA occupying the binding pocket for the ureido oxygen atom of biotin in its complex with wild-type core-streptavidin (transparent atoms and bonds). Hydrogen bonds to the water molecules are shown as yellow broken lines. The binding pocket is enlarged in T7-SA to accommodate the two water molecules.

bind their biotin labels in the normal ligand-binding site.

Materials and Methods

Protein characterization

Building upon Cantor's mature streptavidin gene[20] and cloned by Santambroggio[21] into the pET11b plasmid, we redesigned the gene to incorporate a set of eight unique restriction sites to allow casette mutagenesis. Experimental details, including high level expression, isolation, purification and characterization of mature, full-length streptavidin have been published elsewhere.[22] Active site quantification was achieved using biotin-4-fluorescein using Gruber's protocol.[23]

Crystallization

T7-SA was crystallized using hanging-drop vapor-diffusion techniques. Crystals were obtained by mixing samples of the protein (26 mg/ml) with a 26% saturated ammonium sulfate solution, 0.1 M sodium acetate (pH 4.5), and allowing the drops to equilibrate with a reservoir containing the same ammonium sulfate/sodium acetate solution. The crystals were transferred to 40% saturated ammonium sulfate, 0.1 M sodium acetate (pH 4.5), and 30% (v/v) glycerol in two steps before freezing at 100 K in a nitrogen stream for diffraction data collection.

Data collection

Diffraction data for T7-SA were collected using an in-lab R-Axis IV++ area detector (CuK_α radiation). The space group for the structure is $C2$, with a streptavidin tetramer sitting on a crystallographic 2-fold axis. Two streptavidin subunits are located in the asymmetric unit. The unit cell dimensions are $a=81.70$ Å, $b=82.39$, $c=46.71$, $\beta=103.48°$. The diffraction data were processed with DENZO and merged and scaled with SCALEPACK.[24] Data set statistics are shown in Table 1. The mosaic spread for the crystal was 0.646°.

Structure solution and refinement

The crystal structure of T7-SA was obtained using the molecular replacement program, AMoRe,[25] with a probe structure consisting of a wild-type core-streptavidin monomer. Two subunits were found in the asymmetric unit. The structure was then refined using the SHELXL-97 program.[26] R_{free}[27] was calculated using 10% of the data in the test set. The test set reflections were added to the working set for the final refinement cycles and electron density maps. Distance, planarity, chiral volume, and anti-bumping restraints were applied. Target values for the bond length and bond angle restraints were those assembled by Engh & Huber.[28] Similarity restraints were applied to the atomic isotropic temperature factors. A bulk solvent model was also applied.[29]

SHELXPRO was used for manipulating coordinates and calculating Fourier coefficients for sigma A weighted $|F_o|-|F_c|$ and $2|F_o|-|F_c|$ electron density maps.[30] XtalView[31] was used for graphical evaluation of the model and electron density maps. The final model was validated using PROCHECK.[32] Figures 2–9 were drawn with MOLSCRIPT[33] and Raster3D.[34]

The final model consists of residues 12–45 and 48–159 for one subunit (subunit 1) and residues 14–46 and 49–156 for the second (subunit 2). The N-terminal T7 tag is largely disordered as are portions of the flexible binding loop near residues 45–52. The electron density for the C terminus is well defined for subunit 1, but it is poorer in quality for subunit 2. Two glycerol molecules and a sulfate ion located on a crystallographic 2-fold axis make up the non-protein, non-solvent components of the model. The structural model also contains 272 fully occupied oxygen atoms for water molecules and five half-occupied water molecules. The average B values for the protein are a little high, but this correlates with the weak density and presumed flexibility of the polypeptide loops between the strands of the β-barrel.

The final R value for reflections with $|F_o|>4\sigma(|F_o|)$ is 0.176 while the R for all reflections is 0.179. Table 2 contains refinement statistics for the structure.

Protein Data Bank accession codes

Coordinates and structure factors have been deposited in the Protein Data Bank with identifier 2BC3.

Acknowledgements

This work was partially supported by grant DK49655 from the National Institutes of Health as well as Swiss National Science Foundation grants 620-57866.99 and 200021-105192. We thank C. R. Cantor for the original T7-SA gene.

References

1. Green, N. M. (1963). Avidin. The nature of the biotin-binding site. *Biochem. J.* **89**, 599–609.
2. Sano, T., Vajda, S. & Cantor, C. R. (1998). Genetic engineering of streptavidin, a versatile affinity tag. *J. Chromatog. Ser. B*, **715**, 85–91.
3. Chilkoti, A., Tan, P. H. & Stayton, P. S. (1995). Site-directed mutagenesis studies of the high-affinity streptavidin-biotin complex: contributions of tryptophan residue-79, residue-108, and residue-120. *Proc. Natl Acad. Sci. USA*, **92**, 1754–1758.
4. Freitag, S., Chu, V., Penzotti, J. E., Klumb, L. A., To, R., Hyre, D. *et al*. (1999). A structural snapshot of an intermediate on the streptavidin–biotin dissociation pathway. *Proc. Natl Acad. Sci. USA*, **96**, 8384–8389.
5. Hyre, D. E., Le Trong, I., Freitag, S., Stenkamp, R. E. & Stayton, P. S. (2000). Ser45 plays an important role in managing both the equilibrium and transition state energetics of the streptavidin–biotin system. *Protein Sci.* **9**, 878–885.
6. Sano, T., Pandori, M. W., Chen, X., Smith, C. L. & Cantor, C. R. (1995). Recombinant core streptavidins. *J. Biol. Chem.* **270**, 28204–28209.
7. Hendrickson, W. A., Pahler, A., Smith, J. L., Satow, Y., Merritt, E. A. & Phizackerley, R. P. (1989). Crystal structure of core streptavidin determined from multiwavelength anomalous diffraction of synchrotron radiation. *Proc. Natl Acad. Sci. USA*, **86**, 2190–2194.

8. Weber, P. C., Ohlendorf, D. H., Wendoloski, J. J. & Salemme, F. R. (1989). Structural origins of high-affinity biotin binding to streptavidin. *Science*, **243**, 85–88.
9. Chilkoti, A. & Stayton, P. S. (1995). Molecular-origins of the slow streptavidin–biotin dissociation kinetics. *J. Am. Chem. Soc.* **117**, 10622–10628.
10. Klumb, L. A., Chu, V. & Stayton, P. S. (1998). Energetic roles of hydrogen bonds at the ureido oxygen binding pocket in the streptavidin–biotin complex. *Biochemistry*, **37**, 7657–7663.
11. Schmidt, T. G., Koepke, J., Frank, R. & Skerra, A. (1996). Molecular interaction between the strep-tag affinity peptide and its cognate target, streptavidin. *J. Mol. Biol.* **255**, 753–766.
12. Korndoerfer, I. P. & Skerra, A. (2002). Improved affinity of engineered streptavidin for the strept-tag II peptide is due to a fixed open conformation of the lid-like loop at the binding site. *Protein Sci.* **11**, 883–893.
13. Katz, B. A. & Cass, R. T. (1997). In crystals of complexes of streptavidin with peptide ligands containing the HPQ sequence the pK_a of the peptide histidine is less than 3.0. *J. Biol. Chem.* **272**, 13220–13228.
14. Weber, P. C., Pantoliano, M. W. & Salemme, F. R. (1995). Crystallographic and thermodynamic comparison of structurally diverse molecules binding to streptavidin. *Acta Crystallog. sect. D*, **51**, 590–596.
15. Bayer, E. A., Ben-Hur, H., Hiller, Y. & Wilchek, M. (1989). Postsecretory modifications of streptavidin. *Biochem. J.* **259**, 369–376.
16. Ward, T. R. (2005). Artificial metalloenzymes for enantioselective catalysis based on the noncovalent incorporation of organometallic moieties in a host protein. *Chem. Eur. J.* **11**, 3798–3804.
17. Letondor, C., Humbert, N. & Ward, T. R. (2005). Artificial metalloenzymes based on biotin-avidin technology for the enantioselective reduction of ketones by transfer hydrogenation. *Proc. Natl Acad. Sci. USA*, **102**, 4683–4687.
18. Loosli, A., Rusbandi, U. E., Gradinaru, J., Bernauer, K., Schlaepfer, W., Meyer, M. *et al.* (2006). (Strept) avidin as host for biotinylated coordination complexes: stability, chiral discrimination and cooperativity. *Inorg. Chem.* **45** In the press.
19. Liu, X. & Liu, J. (2005). Signal peptide does not inhibit binding of biotin to streptavidin. *Biotechnol. Letters*, **27**, 1067–1073.
20. Sano, T. & Cantor, C. R. (1990). Expression of a cloned streptavidin gene in *Escherichia coli*. *Proc. Natl Acad. Sci. USA*, **87**, 142–146.
21. Gallizia, A., de Lalla, C., Nardone, E., Santambrogio, P., Brandazza, A., Sidoli, A. & Arosio, P. (1998). Production of a soluble and recombinant streptavidin in *Escherichia coli*. *Protein Expr. Purif.* **14**, 192–196.
22. Humbert, N., Zocchi, A. & Ward, T. R. (2005). Electrophoretic behavior of streptavidin complexed to a biotinylated probe: a functional screening assay for biotin-binding proteins. *Electrophoresis*, **26**, 47–52.
23. Kada, G., Falk, H. & Gruber, H. J. (1999). Accurate measurement of avidin and streptavidin in crude biofluids with a news, optimized biotion-fluorescein conjugate. *Biochim. Biophys. Acta*, **1427**, 33–43.
24. Otwinowski, Z. & Minor, W. (1997). Processing of X-ray diffraction data collected in oscillation mode. *Methods Enzymol.* **276**, 307–326.
25. Navaza, J. (1994). AMoRe—an automated package for molecular replacement. *Acta Crystallog. sect. D*, **50**, 157–163.
26. Sheldrick, G. M. & Schneider, T. R. (1997). SHELXL: High-resolution refinement. *Methods Enzymol.* **277**, 319–343.
27. Brünger, A. T. (1993). Assessment of phase accuracy by cross validation: the free R value. Methods and applications. *Acta Crystallog. sect. D*, **49**, 24–36.
28. Engh, R. A. & Huber, R. (1991). Accurate bond and angle parameters for X-ray protein-structure refinement. *Acta Crystallog. sect. A*, **47**, 392–400.
29. Moews, P. C. & Kretsinger, R. H. (1975). Refinement of the structure of carp muscle calcium binding parvalbumin by model building and difference Fourier analysis. *J. Mol. Biol.* **91**, 201–228.
30. Read, R. J. (1986). Improved Fourier coefficients for maps using phases from partial structures with errors. *Acta Crystallog. sect. A*, **42**, 140–149.
31. McRee, D. E. (1999). XtalView Xfit—a versatile program for manipulating atomic coordinates and electron density. *J. Struct. Biol.* **125**, 156–165.
32. Laskowski, R. A., MacArthur, M. W., Moss, D. S. & Thornton, J. M. (1993). PROCHECK: A program to check the stereochemical quality of protein structures. *J. Appl. Crystallog.* **26**, 283–291.
33. Kraulis, P. J. (1991). Molscript—a program to produce both detailed and schematic plots of protein structures. *J. Appl. Crystallog.* **24**, 946–950.
34. Merritt, E. A. & Bacon, D. J. (1997). Raster3D: Photorealistic molecular graphics. *Methods Enzymol.* **277**, 505–524.

(Received 20 October 2005; received in revised form 25 November 2005; accepted 28 November 2005)
Available online 15 December 2005